

AD-A220 776

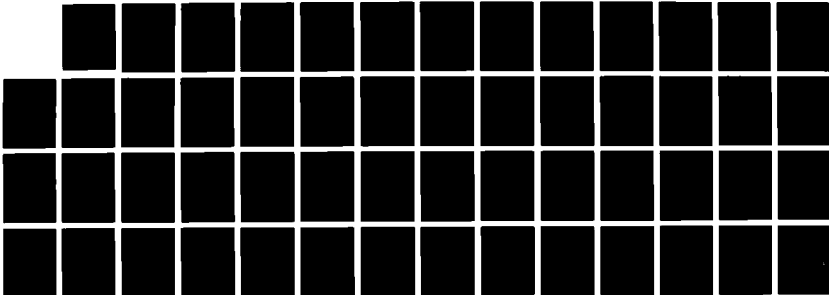
MECHANISMS INDUCING JET ROTATION IN SHEAR-FORMED
SHAPE-CHARGE LINERS(U) ARMY BALLISTIC RESEARCH LAB
ABERDEEN PROVING GROUND MD 5 B SEGLETES MAR 90

2/2

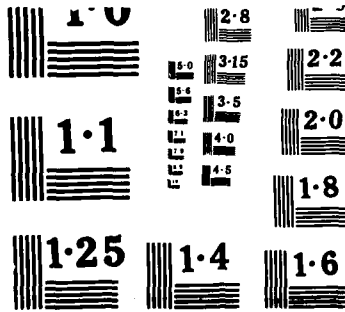
UNCLASSIFIED

F/G 19/1

NL



END
FILMED
DTIC



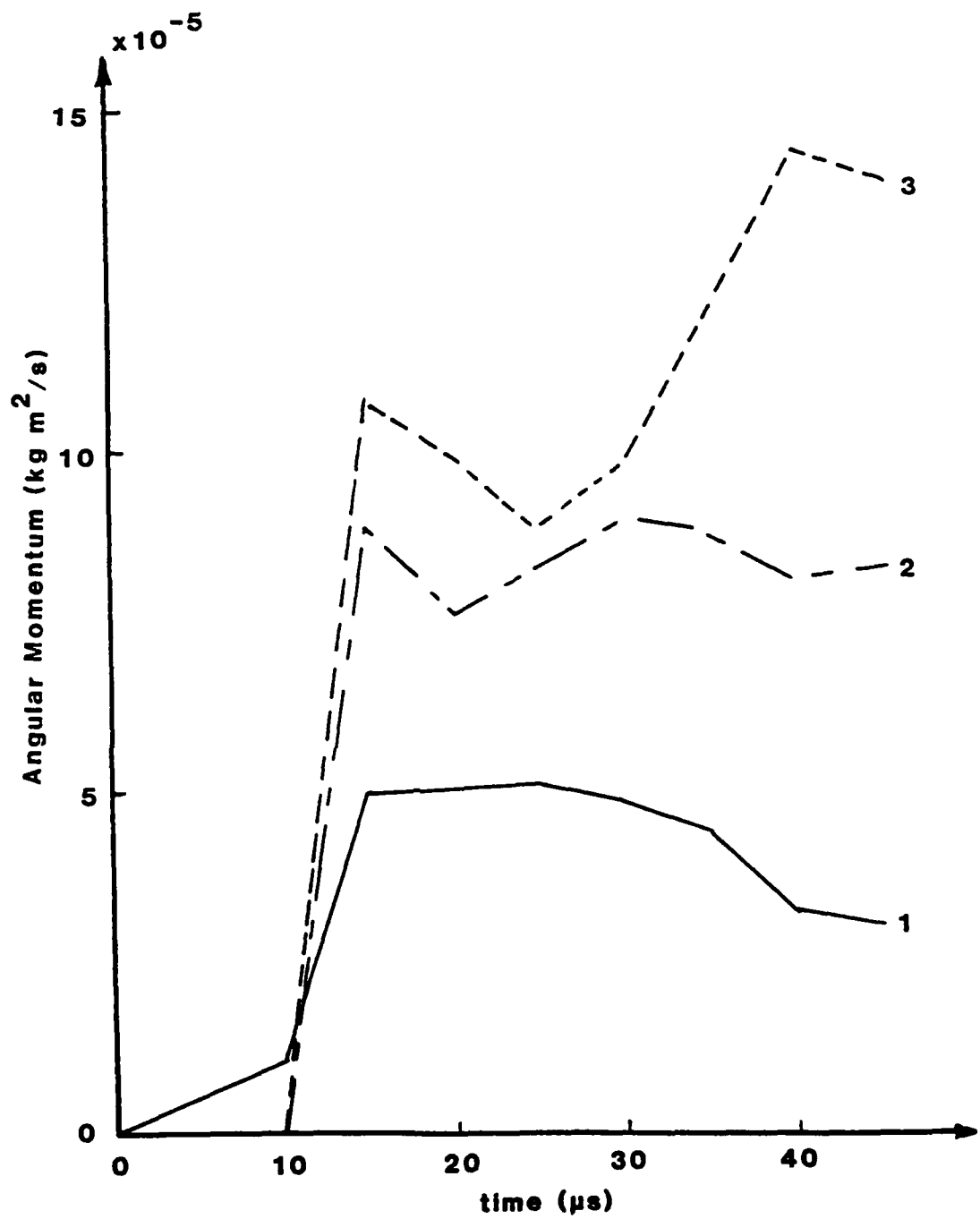


Figure 36. Time history graph of angular momentum for several points on the anisotropic BRL 3.2 liner.

original liner depicted in Figure 37. For points on the inside liner surface (those which end up in the jet), momentum is acquired quite early in the collapse process, and changes little thereafter.

In order to determine the spin compensation frequency of the anisotropic BRL 81 mm liner under study, other numerical simulations were performed in which initial charge spin was placed on the liner (in a direction opposite the observed anisotropy induced spin). By observing the angular velocity characteristics of the resultant jets, it was determined that the spin compensation frequency for the charge under study is indeed the expected value of 35 rps. A plot of the jet spin versus axial particle velocity is shown in Figure 38 for both the unspun anisotropic charge originally simulated and the same charge rotated 35 rps. It is seen that at the spin compensation frequency, the angular velocity of the jet is nearly negligible.

It was shown earlier from analytical considerations, if the θ direction is a preferred material direction (so called r-z anisotropy, since the anisotropy angle Γ lies in the r-z plane), that induced jet rotation was not possible. However, it was shown, if the radial r direction was a preferred material direction, that induced θ motion was possible. As such, a final axisymmetric simulation was performed of the collapsing liner with z- θ anisotropy. The results indicate small, random, material rotations in and out of the r-z plane, but more than an order of magnitude below the results of r- θ anisotropy discussed earlier. Though there is indeed variation of properties in the r- θ plane with the case of z- θ anisotropy, a transformation of the strengths into the laboratory r-z- θ coordinate system reveals that strength extrema in the r- θ plane coincide exactly with r and θ coordinate directions. Under these conditions, there is no tendency for r- θ shear coupling, and thus any coupling must be z- θ coupling. Apparently, the stresses tending to produce out of plane rotations from z- θ coupling are not mutually constructive as in the case of r- θ anisotropy, and compensation therefore does not result.

5. CONCLUSIONS AND RECOMMENDATIONS

This report has addressed several mechanisms by which rotation might be induced in a jet of a stationary shaped charge which employs a shear-formed liner. In particular, two modes of residual stress relief have been examined, along with elastic and plastic mechanical anisotropy. Results indicate that plastic anisotropy is the only mechanism

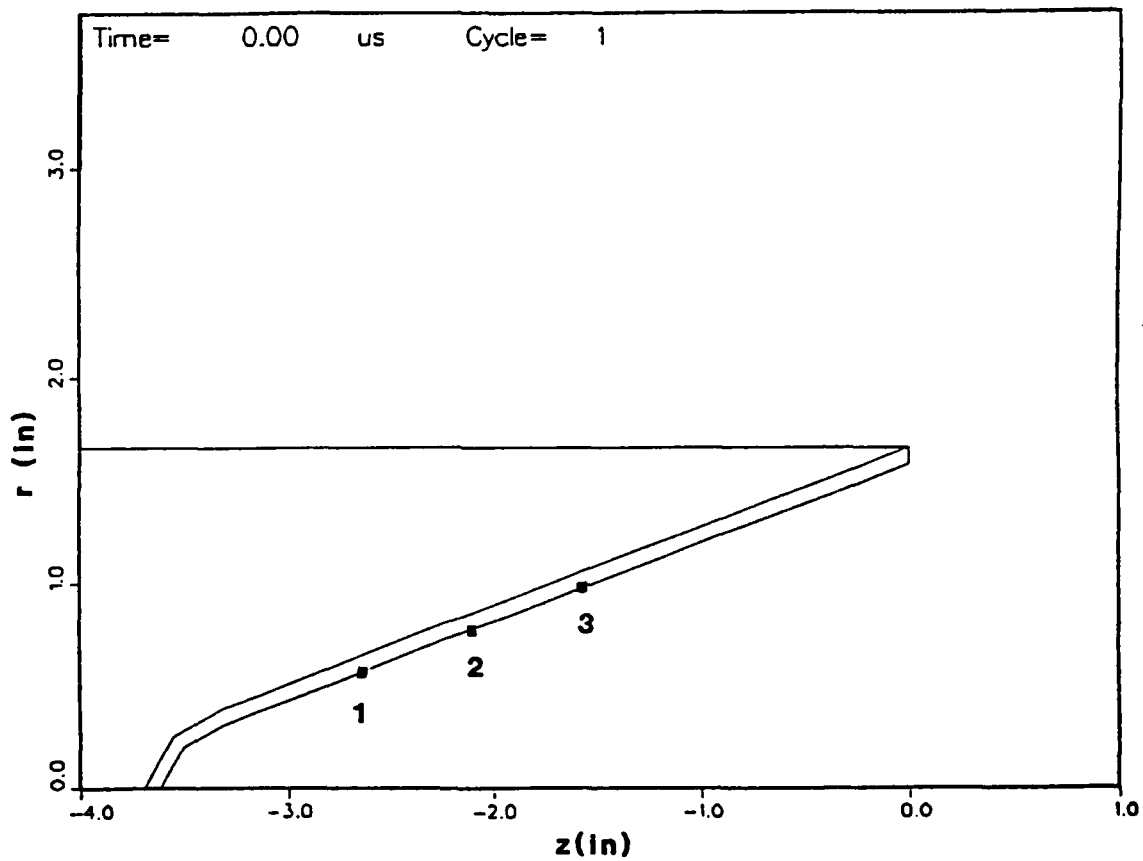


Figure 37. Initial outline of simulation geometry, depicting material points whose angular momentums have been traced in time.

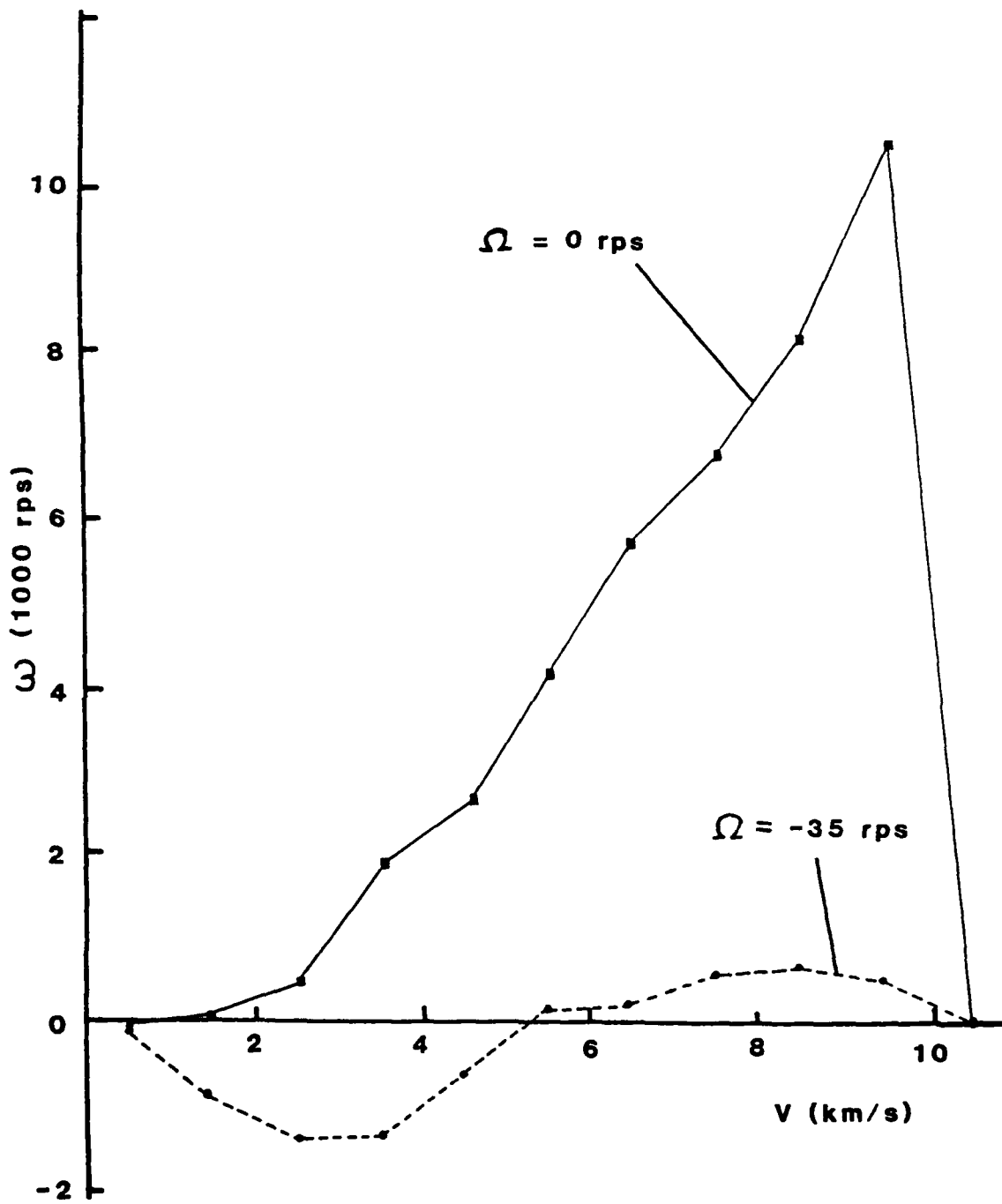


Figure 38. Jet spin versus axial jet velocity for unspun charge and charge spun at 35 rps opposite direction of spin compensation.

studied which is capable of producing jet rotation rates of the magnitude observed experimentally in shear-formed shaped-charge liners. In support of the report, several advances were made in related areas.

A computational anisotropic formulation was developed⁴⁴ which offers significant benefits over previous anisotropic formulations, in terms of computational accuracy. The computational formulation, being the first treatment of anisotropy from a deviator stress/strain perspective, provides an enhanced understanding of the mechanics of anisotropic deformation.

In a related effort, a means was developed to track the rotation of computational elements out of the r - z plane. The formulation is instrumental in performing anisotropic computational simulations in axisymmetry mode.

The analytical model developed to predict the spin compensation resulting from plastic anisotropy was compared to computational results of anisotropic liner collapse. The 2-D anisotropic plane stress and axisymmetric computational results match the analytical predictions in both magnitude and character, thereby supporting the validity of the analytical model of anisotropic spin compensation.

The plastic potential gradient of an anisotropic material was derived for a specific non-preferred coordinate system, resulting from a single coordinate rotation. The resulting plastic flow rule has been expressed in terms of the preferred coordinate system potential gradient augmented by a deviation potential gradient. Though the potential is not derived for arbitrary (three parameter) rotations from the preferred coordinate system, it nonetheless provides a useful tool for examining the effect of coordinate system rotations on shear coupling ratios.

Future examination of the report topic would be quite valuable from the perspective of material characterization. As it was, anisotropic material parameters for shear-formed liners were extrapolated from incomplete rotary forged tensile data. In the long term, the acquisition of macroscopic mechanical properties (e.g., yield strengths) of liner material from metallurgical considerations, though beyond the scope of the current research, would provide the vital link which might allow one to choose the metal forming process necessary to produce a liner of the proper anisotropic characteristics. Through this means, one

should be able predict the spin compensation ability of the shaped-charge liner in advance of manufacture. In the near term, the development of better methods to acquire the necessary macroscopic mechanical properties of liner material would permit one to predict spin compensation behavior of a liner without actually conducting a costly experimental shaped-charge testing program.

6. REFERENCES

1. Walters, W., "Fundamentals of Shaped Charges," Fundamentals of Shaped Charges, Vol. 1, Baltimore: Computational Mechanics Associates, pp. 20-40, 1988.
2. Weickert, C.A., "Spinning Self-Forging Fragments and Shaped Charges," Ph.D. Thesis, Drexel University, June 1986.
3. Birkhoff, G., MacDougall, D.P., Pugh, E.M., and Taylor, Sir G., "Explosives with Lined Cavities," *Journal of Applied Physics*, 19:6, pp. 563-582, June 1948.
4. Eichelberger, R.J., "Spin Compensation," Critical Review of Shaped Charge Information, BRL Report 905, Chapter VIII, pp. 215-253, May 1954.
5. Zernow, L., "The Effect of Rotation Upon Shaped Charge Jets," Critical Review of Shaped Charge Information, BRL Report 905, Chapter VII, pp. 177-213, May 1954.
6. Zernow, L. and Simon, J., "Flash Radiographic Study of Spin Compensation with 105 mm Fluted Liners," *Shaped Charge Journal*, 1:1, July 1954.
7. Zernow, L. and Simon, J., "Flash Radiographic Study of Spin Compensation in Shear Formed Liners (ITE)," *Shaped Charge Journal*, 1:1, July 1954.
8. Simon, J. and Zernow, L., "'Metallurgical' Spin Compensation in Smooth Electroformed Liners," *Shaped Charge Journal*, 1:1, July 1954.
9. Litchfield, E.L. and Eichelberger, R.J., "Performance of 57 mm Fluted Cones Made for Dynamic Testing," *Shaped Charge Journal*, 1:2, October 1954.
10. Becker, K.R., "57 mm Fluted Liners," The Ordnance Corps Shaped Charge Research Report, BRL 4-55, October 1955.
11. Becker, K.R., "75 mm Fluted Liners," The Ordnance Corps Shaped Charge Research Report, BRL 4-55, October 1955.
12. Simon, J., "Flash Radiographic Study of Spin Compensation With 105 mm Fluted Liners," The Ordnance Corps Shaped Charge Research Report, BRL 4-55, October 1955.
13. Simon, J. and Zernow, L., "Flash Radiographic Study of Spin Compensation in 105 mm Copper Liners Manufactured by Controlled 'Spinning'," The Ordnance Corps Shaped Charge Research Report, BRL 4-55, October 1955.

14. DiPersio, R. and Simon, J., "An Empirical Approach to the Design of a Spin Compensating Shaped Charge," BRL Memorandum Report 1251, February 1960.
15. Zernow, L. and Simon, J., "High Strain Rate Plasticity of Liner Materials and Jet Behavior," BRL Report 954, August 1955.
16. Simon, J., DiPersio, R., and Eichelberger, R.J., "Shaped Charge Performance With Linear Fluted Liners," BRL Memorandum Report 1231, September 1959.
17. Simon, J. and Zernow, L., "Flash Radiographic Study of Certain Anomalous Electroformed Liners for Shaped Charges," BRL Memorandum Report 892, June 1955.
18. Simon, J. and Martin, T.K., "Spin Compensation of Shaped Charge Liners Manufactured by the Rotary Extrusion Process," BRL Memorandum Report 1181, December 1958.
19. Glass, C.M., Gainer, M.K., and Moss, G.L., "Effects of Anisotropies in Rotary Extruded Liners," BRL Report 1084, November 1959.
20. Gainer, M.K. and Glass, C.M., "A Study of Metallurgical Effects in High Velocity Deformation of Copper Using Rotary Extruded Liners," BRL Report 1167, May 1962.
21. Weickert, C.A. and Chou, P.C., "Shaped Charge Spin Compensation with Fluted Liners," Proc. 9th International Symposium on Ballistics, Shrivenham, UK, 29-30 April, 1 May, 1986.
22. Karpp, R. and Simon, J., "An Estimate of the Strength of a Copper Shaped Charge Jet and the Effect of Strength on the Breakup of a Stretching Jet," BRL Report 1893, June 1976.
23. Dyna East Corporation, "Study of Jet Breakup and the Collapse of Spinning Liners," Quarterly Tech. Report for Contract DAAK11-78-C-0101, March 1979.
24. Timoshenko, S.P. and Goodier, J.N., Theory of Elasticity, 3rd ed. New York: McGraw Hill Book Co., Inc., 1970.
25. Zernow L. and Simon, J., "Flash Radiographic Study of Special Liners for Shaped Charges," BRL Report 936, June 1955.
26. Poulter, T., "A Study of Material for Shaped Charges: The Effect of Crystal Orientation on Jet Formation," Tech. Report No. 3, Poulter Laboratories, SRI Project No. GU-863 for BRL Contract No. DA-04-200-ORD-257, 15 February 1955.
27. Witt, F., "X-ray Studies on the Flared Cone Component for Metal Parts Assembly M456A1E1," FA-TR-74046, December 1974.
28. Witt, F., "X-ray Studies of Belgian Produced 105 mm HEAT-T-M456 Spin Compensated Shaped Charge Liners," FA-TR-75001, January 1975.
29. Feng, C., Witt, F., and Lee, F., "A Metallurgical Evaluation of Shear-Spun and Deep Drawn Copperhead Liners," ARDC Report MMB-57-80, 1980.

30. Feng, C., Lee, F., and Witt, F., "Metalurgical Comparisons Between Two Starting Stock Materials Used in the Improved TOW Shaped Charge Liner," ARDC Report MMB-18-81, March 1981.
31. Witt, F., US Army Armament Research, Development and Engineering Center, Picatinny Arsenal, NJ, private communication, December 1987.
32. Majerus, J., Golaski, S., and Merendino, A., "Influence of Liner Metallurgy, Apex Configuration and Explosive/Metal Bond Strength upon Performance of Precision Shaped-Charges," BRL Report ARBRL-TR-02451, December 1982.
33. Crilly, M., et al., "Evaluation of the Effect of Liner Grain Size on Shaped-Charge Performance," Project M13, Drexel University Senior Design Report, May 1984.
34. Nuclear Metals, Inc., "Material Certification and Dimensional Inspection Data for Ballistic Research Laboratory Contract No. DAAD05-85-C-4156," June 27, 1985.
35. Duffy, M. and Golaski, S., "Effect of Liner Grain Size on Shaped Charge Jet Performance and Characteristics," BRL Report BRL-TR-2800, April 1987.
36. Wenk, H.R., ed. Preferred Orientation in Deformed Metals and Rocks: An Introduction to Modern Texture Analysis, Orlando: Academic Press, 1985.
37. Cullity, B.D., Elements of X-ray Diffraction, Reading: Addison-Wesley, 1978.
38. Schiferl, S., Los Alamos National Laboratory, Los Alamos, NM, Private Communication, February 1988.
39. Hill R., The Mathematical Theory of Plasticity, London: Oxford Press, 1950.
40. Franz, R., US Army Ballistic Research Laboratory, Aberdeen Proving Ground, MD, Private Communication, January 1987.
41. Chou, A. and Labriola, M. Jr., "Rotary Forging - A Precision Process," Mechanical Engineering, 107:3, pp. 73-77, March 1985.
42. Baldwin, W.M., Jr., "Effect of Rolling and Annealing upon the Crystallography, Metallography, and Physical Properties of Copper Strip," Proc. 9th Sagamore Army Materials Research Conference, Raquette Lake, NY, August 28-31, 1962.
43. Flis, W.J., Miller, S., and Clark, W.J., "DEFEL: A Finite-Element Hydrodynamic Computer Code," Dyna East Technical Report DE-TR-84-05, November 1984.
44. Segletes, S., "Deviatoric Constitutive Relationship for Anisotropic Materials," BRL Report BRL-TR-2825, June 1987.
45. Baker, P., US Army Ballistic Research Laboratory, Aberdeen Proving Ground, MD, Private Communication, September 1988.
46. Dyna East Corporation, "DEFEL User's Manual," Dyna East Corporation Technical Report DE-TR-85-02, Second Revision, May 1985.

47. Johnson, G.R., "EPIC-2, A Computer Program for Elastic-Plastic Impact Computations Plus Spin," Final Report, Contract No. DAAD05-77-C-0730, US Army Ballistic Research Laboratory, December 1977.
48. Walsh, J.M. et al., "HELP, A Multi-Material Eulerian Program for Compressible Fluid and Elastic-Plastic Flows in Two Space Dimensions and Time." Vols. I and II, Systems, Science and Software, 3SR-350, June 1970.
49. Johnson, W. and Mellor, P.B., Engineering Plasticity, Chichester: Ellis Horwood, Chapter 5, 1983.
50. Hageman, L.J. et al., "HELP, A Multi-Material Eulerian Program for Two Compressible Fluid and Elastic-Plastic Flows in Two Space Dimensions and Time," Systems, Science and Software, SSS-R-75-2654, July 1975.
51. Vavrick, D.J. and Johnson, G.R., "Dynamic Analysis of Elastic-Plastic Anisotropic Solids," Honeywell Internal Report, Contract No. DAAK11-78-C-0010, US Army Ballistic Research Laboratory, October 1980.
52. Wu, L., Drexel University, Philadelphia, PA, Private Communication, November 1985.

INTENTIONALLY LEFT BLANK.

APPENDIX A:
DEVIATORIC CONSTITUTIVE RELATION
FOR ANISOTROPIC MATERIALS

INTENTIONALLY LEFT BLANK.

APPENDIX A:
DEVIATORIC CONSTITUTIVE RELATION
FOR ANISOTROPIC MATERIALS

The information presented in this appendix is a summary of that found in reference 44. It is presented here to assist the reader in understanding the computational techniques developed for use in the current research.

A.1 Introduction.

It is desired to improve upon the ability to describe the behavior of anisotropic media subjected to large pressures, as is the case for hypervelocity impact. It is believed that expressing the anisotropic constitutive relationship in a form that makes use of the deviatoric stress and strain tensors provides for a better description of anisotropic materials whose compressibility is permitted to vary with volumetric strain. The deviatoric stress technique is used routinely in many impact codes for describing isotropic behavior⁴⁶⁻⁴⁸, and is described in many books on elasticity and plasticity.^{24,49} Anisotropic schemes have also been developed for various impact codes⁵⁰⁻⁵¹ which calculate a deviatoric stress. However, the deviatoric stress is expressed in terms of a total strain and the bulk modulus. In a true deviatoric formulation, deviatoric stress is expressed only in terms of deviatoric strain, and compressibility affects only the equation of state, not the deviatoric stress/strain relation.

An anisotropic formulation is proposed which satisfies the condition of reducing to Hooke's Law/Prandtl Reuss Flow Rule when employing the constraint of constant compressibility and isotropy, but which conveniently allows for anisotropy and variable compressibility. Additionally, the formulation is amenable for inclusion into existing impact codes which presently use the deviatoric stress technique for isotropic materials. The scheme also provides an improved technique for calculating hydrostatic pressure which is less prone to error than existing techniques. Finally, it is hoped that the formulation provides an enhanced physical interpretation on the behavior of anisotropic materials which might otherwise be lacking.

A.2 Background.

The constitutive relationship for any elastic material may be represented in contracted form as

$$\sigma_i = C_{ij} \varepsilon_j \quad (A-1)$$

where σ_i and ε_j represent the six independent stress and strain components, and C_{ij} is the modulus matrix. The contracted form of the constitutive relation is used for the sake of simplicity, but the tensorial components of the contracted form are defined as follows:

$$\sigma_i = (\sigma_{11} \ \sigma_{22} \ \sigma_{33} \ \sigma_{23} \ \sigma_{13} \ \sigma_{12})$$

$$\varepsilon_i = (\varepsilon_{11} \ \varepsilon_{22} \ \varepsilon_{33} \ \varepsilon_{23} \ \varepsilon_{13} \ \varepsilon_{12})$$

In general, C_{ij} may be a function of σ , ε , $\dot{\varepsilon}$, etc. However, it is somewhat unwieldy as such, and is sometimes considered to be constructed of constants, which produces the familiar Hooke's Law. One reason why the deficiency of Hooke's Law becomes apparent experimentally under large pressures is that the bulk modulus of the material is quite different from the material's low stress value.

For isotropic materials, this problem has been computationally circumvented by the introduction of the deviatoric stress and strain tensors. These tensors differ from the absolute stress/strain tensors in that the normal components of stress and strain are decremented by the average of the normal stresses and strains respectively. In this way, the deviatoric quantities represent deviation from a hydrostatic condition, while the relationship existing between the average stress (negative of pressure) and average strain (volumetric dilatation) is an equation of state. Since experimental evidence reveals that the compressibility of many materials changes under large pressures, the deviatoric formulation suggests that while the simplicity of Hooke's Law (constant coefficients) might possibly be retained for computation of the deviatoric stresses and strains, a more accurate scalar equation of state should simultaneously be employed to account for non-linear compressibility effects.

A.3 Elastic Deviatoric Anisotropy.

While the mathematics of the constant coefficient constitutive relationship for anisotropic materials is well understood, the casting of these rules into a deviatoric format is not nearly as straightforward as it is for isotropic materials. Difficulties arise because of two primary differences in the behavior of anisotropic materials with respect to that of isotropic materials:

a. under hydrostatic pressure, strain is not uniform in all three directions of the material coordinates, and

b. except under restrictive modulus conditions, deviatoric strain will produce volumetric dilatation (i.e., two different stress states with the same pressure will produce different dilatations in the material).

Decomposition of the stress and strain tensors into their hydrostatic and deviatoric components yields:

$$s_i = \sigma_i - \bar{\sigma}_i \quad (\text{A-2})$$

$$e_j = \varepsilon_j - \bar{\varepsilon}_j \quad (\text{A-3})$$

where $\bar{\sigma}_i$ are all equal to the components of hydrostatic stress ($\bar{\sigma} = (\sigma_1 + \sigma_2 + \sigma_3)/3$) for normal stress components and equal to zero for the shear stress components. The term $\bar{\varepsilon}_j$ represents the normal strains due to hydrostatic stress. One may acquire upon substitution into equation (A-1):

$$(s_i + \bar{\sigma}_i) = C_{ij} (e_j + \bar{\varepsilon}_j) \quad (\text{A-4})$$

where barred quantities represent conditions resulting from a hydrostatic pressure, s_i and e_j are the deviatoric stresses and strains respectively, and C_{ij} is the modulus matrix. Unlike the isotropic materials in which a hydrostatic pressure produces a uniform dilatation in all three coordinate directions, hydrostatic strain for an anisotropic material is non-uniform. Therefore, if one defines the deviatoric components of stress and strain to be the total stress/strain components decremented by an amount which would result from a hydrostatic

stress state, one can conclude (per condition "a" above) that there is a unique hydrostatic strain component associated with all three directions in the material coordinates (the coordinate system which produces no shear coupling). Equation (A-4) may be decoupled to give a hydrostatic equation

$$\bar{\sigma}_i = C_{ij} \bar{\epsilon}_j \quad (\text{A-5})$$

and a deviatoric relationship void of hydrostatic terms:

$$s_i = C_{ij} e_j \quad (\text{A-6})$$

For the sake of clear visualization, the formulation will be described for transverse isotropy, though extension to orthotropy is straightforward⁵². Figure A-1 depicts material elements from an anisotropic body whose material (preferred) coordinate systems differ from the laboratory frame of reference. The preferred coordinate system is the reference frame in which the constitutive relation reduces to its most simple form. Figure A-2 shows properties of the preferred transversely isotropic material frame. Mechanical properties are invariant with respect to reference frame rotations that are confined to the plane of isotropy. As such, a certain symmetry of mechanical properties exist in transversely isotropic materials which are absent in orthotropic materials. The proposed model will be described in the material (preferred) coordinate system. Solutions of problems in which the laboratory frame and the material frame do not coincide pose no problem if one first transforms stress and strain to the material frame.

Under the influence of a purely hydrostatic stress state (and assuming the moduli to be constant), there will be a constant ratio between the anisotropic (longitudinal) strain $\bar{\epsilon}_1$ and the transversely isotropic planar strain $\bar{\epsilon}_2$. Defining the ratio in terms of material compliances S_{ij} (where $S_{ij} = (C_{ij})^{-1}$):

$$K_\epsilon = \frac{\bar{\epsilon}_1}{\bar{\epsilon}_2} = \frac{S_{11} + 2S_{12}}{S_{22} + S_{12} + S_{23}} \quad (\text{A-7})$$

it is seen that this parameter (K_ϵ) reduces to a value of unity for isotropy, where S_{11} will equal S_{22} , and S_{12} will equal S_{23} .

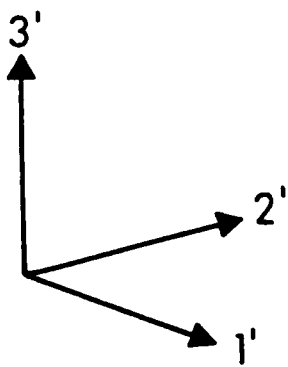
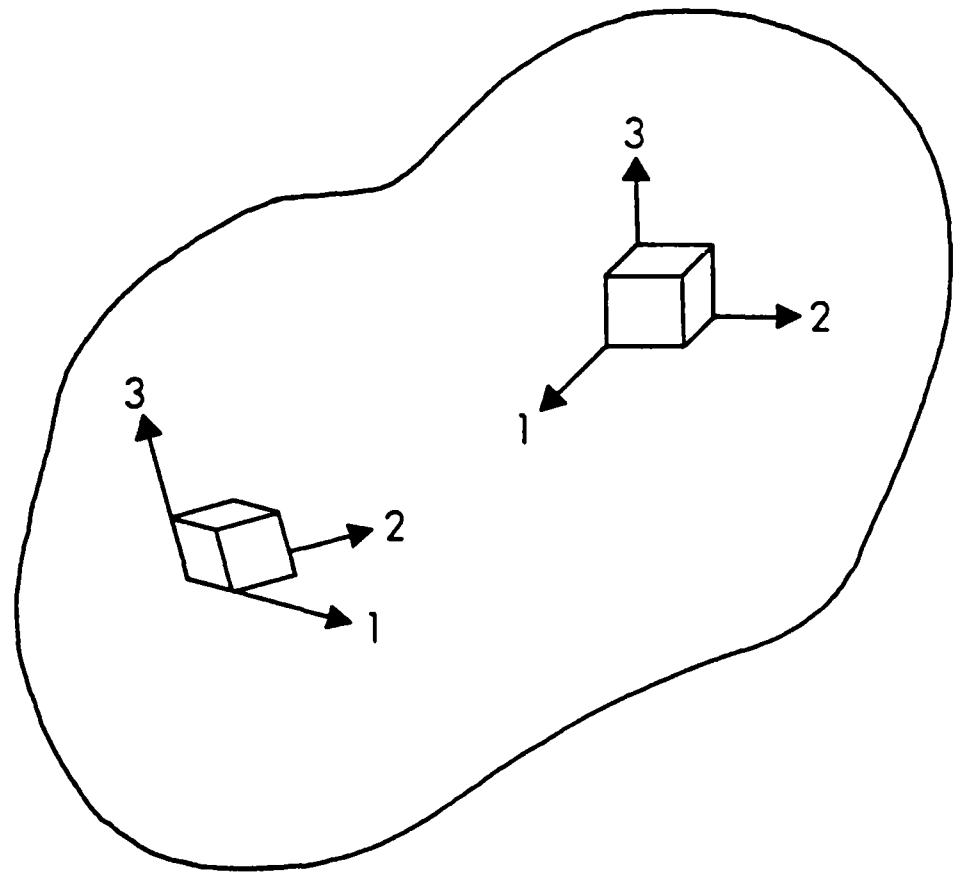
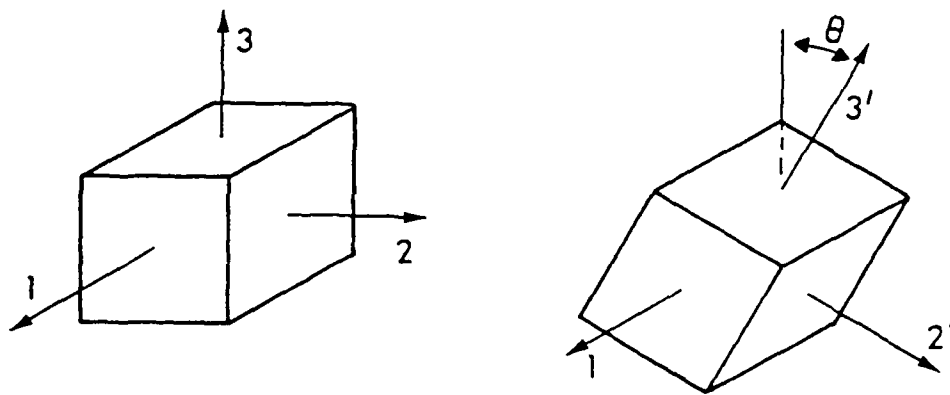


Figure A-1. Schematic depiction of general anisotropic body, where principal material directions are not generally aligned with laboratory axes.



$$\nu_{13} = \nu_{13'}, G_{13} = G_{13'}, E_3 = E_{3'}, Y_3 = Y_{3'}, Y_{13} = Y_{13'}$$

When $\theta = 90^\circ$, it follows that

$$\nu_{12} = \nu_{13}, G_{12} = G_{13}, E_2 = E_3, Y_2 = Y_3, Y_{12} = Y_{13}$$

Figure A-2. Transversely isotropic material properties are derivable from orthotropic properties, when plane of material symmetry is assumed.

Using the definition that deviatoric stress is that part of the stress tensor which deviates from the hydrostatic stress condition, one can conclude that the deviatoric stress has no hydrostatic component

$$s_1 + s_2 + s_3 = 0 \quad (\text{A-8})$$

One may substitute the deviatoric constitutive relation, equation (A-6), to acquire

$$K_\sigma e_1 + e_2 + e_3 = 0 \quad (\text{A-9})$$

where K_σ physically represents the ratio of longitudinal and transverse stress under conditions of uniform strain ($\epsilon_1 = \epsilon_2 = \epsilon_3$), and is given by

$$K_\sigma = \frac{C_{11} + 2C_{12}}{C_{22} + C_{12} + C_{23}} \quad (\text{A-10})$$

As a result, the sum of the three normal deviatoric strain increments is not generally zero, but rather equals a deviatoric dilatation (\bar{e}). The significance of this term is that a state of stress whose average normal value is zero can produce volumetric change on an element with respect to that element's stress free volume.

If one wishes to convert a given elastic strain state (ϵ_i) into the elastic deviators (e_i), elastic deviatoric dilatation (\bar{e}), and the hydrostatic strain components ($\bar{\epsilon}_i$), the following nine equations given below may be used for a transversely isotropic material (whose plane of isotropy is the 2-3 plane):

$$e_1 = \epsilon_1 - \bar{\epsilon}_1 \quad (\text{A-3a})$$

$$e_2 = \epsilon_2 - \bar{\epsilon}_2 \quad (\text{A-3b})$$

$$e_3 = \epsilon_3 - \bar{\epsilon}_2 \quad (\text{A-3c})$$

$$e_4 = \epsilon_4 \quad (\text{A-3d})$$

$$e_5 = \varepsilon_5 \quad (\text{A-3e})$$

$$e_6 = \varepsilon_6 \quad (\text{A-3f})$$

$$\bar{e}_1 = e_1 + e_2 + e_3 \quad (\text{Dilatation of Deviatoric Strain}) \quad (\text{A-11})$$

$$\bar{\varepsilon}_1 = K_c \bar{\varepsilon}_2 \quad (\text{Non-uniform hydrostatic strain}) \quad (\text{A-7})$$

$$K_\sigma e_1 + e_2 + e_3 = 0 \quad (\text{Assures that deviatoric stress has no hydrostatic component}) \quad (\text{A-9})$$

Finally, the use of the deviatoric constitutive relation, equation (A-6) hinged upon the satisfaction of equation (A-5). Inverting equation (A-5) into compliance form and summing the three equations for normal strain yields upon reduction:

$$\bar{\sigma} = \tilde{K} (\varepsilon_1 + \varepsilon_2 + \varepsilon_3 - \bar{e}) \quad (\text{A-12})$$

where \tilde{K} is a true material property which will be called the effective bulk modulus of the material (it equals the reciprocal of the sum of the nine normal compliance matrix components), and $(\varepsilon_1 + \varepsilon_2 + \varepsilon_3)$ is the total volumetric dilatation of the material element. This effective modulus, unlike the bulk modulus, is independent of deviatoric stress in anisotropic materials. The bulk modulus reduces to the effective bulk modulus only when the deviatoric dilatation \bar{e} equals zero. This condition occurs under either of the following conditions: the material is isotropic, or the loading is purely hydrostatic.

It was mentioned previously that the empirical relation between dilatation and pressure is not a linear one. One advantage of the deviatoric formulation lies in the ability to arbitrarily make the hydrostatic relation non-linear while retaining the linear simplicity of Hooke's Law for the deviatoric portion of the constitutive relation. Though this ad hoc procedure does not theoretically follow as an extension to Hooke's Law, it does permit the code user to more flexibly model the empirical behavior of the material.

There are also codes employing the incremental strain approach which use a formulation employing deviatoric stress, though the formulation can not be termed deviatoric. The form of the relation used by the HELP code⁵⁰ is

$$\Delta s_i = \begin{cases} C_{ij} \Delta \epsilon_j - 3K (\Delta \epsilon_1 + \Delta \epsilon_2 + \Delta \epsilon_3) , & i=1,2,3 \\ C_{ij} \Delta \epsilon_j & i=4,5,6 \end{cases} \quad (A-13)$$

where K is identified as the bulk modulus which presumably can be made dependent on dilatation (and therefore hydrostatic stress). In this way, the formulation may also provide the flexibility of a truly deviatoric formulation. However, equation (A-13) is not truly a deviatoric relation, since the deviatoric stress increment is not related to deviatoric strain increment, but rather is expressed in terms of the total strain increment. The system of equations presently proposed, equations (A-6) and (A-12), are thus more attractive in a theoretical sense. Similarly, it has already been pointed out that the bulk modulus (as opposed to the effective bulk modulus derived in equation (A-12)) is functionally dependent on deviatoric stress, and in this sense equation (A-13) will exhibit flawed behavior if the deviatoric variation in bulk modulus is not modeled. Finally, the flexibility afforded in equation (A-13) by allowing the bulk modulus to vary with hydrostatic stress has the disturbing effect that the resulting sum of the normal stress deviators is not generally zero. If this interpretation of the HELP⁵⁰ is correct, the use of the term stress deviators to describe the left hand side of equation (A-13) is not even justified.

EPIC⁵¹ use a form similar to equation (A-13) except that K is defined in such a way as to force the sum of the normal stress deviators to zero. This ad hoc procedure will coincidentally mimic the behavior of equation (A-6), though the formulation is in error during the subsequent hydrostatic stress calculation by not accounting for the deviatorically induced dilatation ($\bar{\epsilon}$).

Additional advantages afforded by the proposed formulation when using a code which employs an incremental strain approach, may be seen by comparing the proposed algorithm specifics with that of the prior formulation used in HELP⁵⁰. The proposed formulation takes strain increments, and decomposes them into hydrostatic and deviatoric components. Equation (A-6) is used in an incremental way to update deviatoric stress. If

the hydrostatic strain increments are summed and remembered, equation (A-12) may be used to evaluate the hydrostatic stress value directly. If the hydrostatic stress is a function of volumetric dilatation only, then errors introduced into the calculation of hydrostatic stress are machine precision dependent, but not algorithm dependent. That is to say, errors in the calculation of hydrostatic pressure are insensitive to the size of the hydrostatic strain increment.

On the other hand, an incremental stress formulation like that proposed for HELP⁵⁰ experiences errors which are dependent on hydrostatic strain increment size (which is proportional to the calculation timestep size), if variable compressibility is employed. For example, use of equation (A-13) as described for materials with variable compressibility requires that some sort of average compressibility be calculated for the time increment in question. As shown in Figure A-3, the average bulk modulus depends not only on the total element dilatation, but also on the size of the strain increment (since dilatation changes with strain increment). Therefore, the accuracy of such a scheme is limited by the integration step size regardless of machine precision. Presumably, this problem can be avoided if one replaces the modulus dilatation product at the end of equation (A-13) with a $\Delta\bar{\sigma}$ term, where the $\Delta\bar{\sigma}$ term is directly obtainable knowing the previous and present cycles' average stress.

However, many non-linear equations of state that are routinely employed in impact codes like HELP⁵⁰ show a dependence of hydrostatic pressure on internal energy. Under such conditions, this dependence of pressure on energy must effectively be reflected in equation (A-13) for consistency to be maintained. However, since internal energy is affected by the work done by the internal stresses (which include deviatoric stresses), a coupling of internal energy, pressure, and deviatoric stresses exists. No simple means exists to solve this set of equations simultaneously, and a lengthy iterative process becomes necessary. No mention of such coupling and/or iteration was made⁵⁰. Thus, it can be seen that equation (A-13) suffers many drawbacks which make its use less desirable than the proposed method given by equations (A-6) and (A-12) in which the deviatoric relations are free of hydrostatic terms.

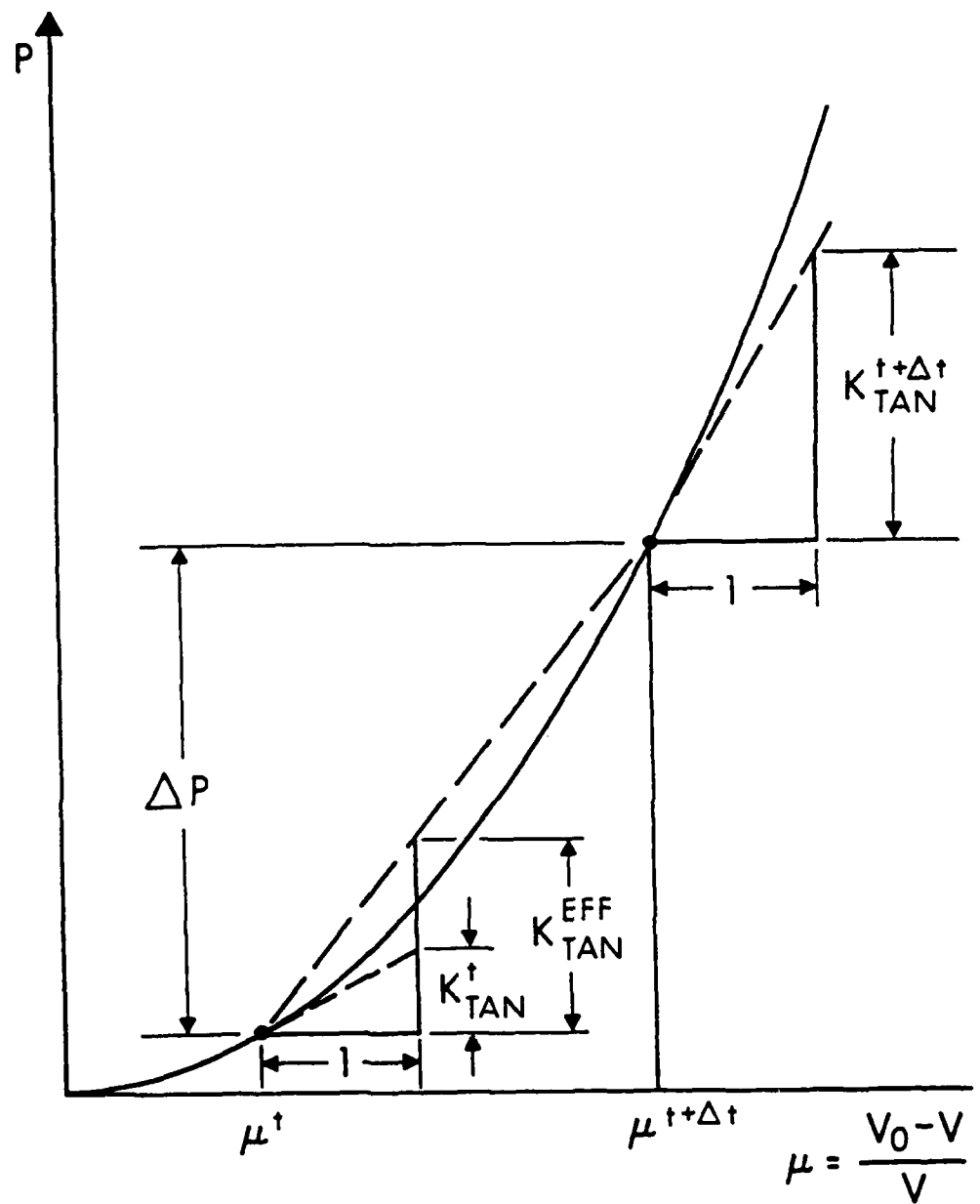


Figure A-3. Error in computation of hydrostatic pressure is introduced if tangent modulus is employed.

In summary, the steps proposed for deducing elastic anisotropic deviators in equations (A-6) and (A-12) follow closely those for isotropic materials in the following ways:

- a. deviatoric stress is expressible totally in terms of deviatoric strain, and
- b. pressure is expressible totally in terms of dilatations.

The differences from the isotropic formulation are:

- a. the matrix relating deviatoric stress to deviatoric strain is not diagonal in the anisotropic case, and
- b. the total volumetric dilatation must be modified by the deviatorically induced dilatation when calculating the pressure.

A.4 Plastic Deviatoric Anisotropy.

The anisotropic equivalent to the Prandtl-Reuss flow rule of plasticity can be similarly cast into a deviatoric form. Stress behavior of yielding material is governed primarily by the nature of the yield surface, which defines the allowable stress states of the material and subsequent plastic flow properties. In general, only a portion of a post-elastic strain increment ($\Delta\varepsilon_j^I$) contributes to changing the stress. That portion is designated the elastic strain increment ($\Delta\varepsilon_j$). The remaining portion of the strain increment is designated the plastic strain increment ($\Delta\varepsilon_j^P$). This decomposition of the strain increment is governed by two rules:

- a. an infinitesimal plastic strain increment vector must be normal to the yield surface at the stress state under consideration, and
- b. a stress increment vector tending to go outside of the yield surface can at most move tangentially to the yield surface at the stress state under consideration.

Because of the linearity of the equations governing the conversion from absolute elastic strain (ε_j) to deviatoric elastic strain ($e_j, \bar{e}, \bar{\varepsilon}_j$), one is assured that by decomposing

the elastic strain increment into any two arbitrary divisions, the sum of the two converted strain divisions equals the conversion of the strain division sum. This rule becomes handy for impact code implementation if the two strain divisions are taken as the total strain increment and the negative of the plastic strain increment (the sum of which add up to the elastic strain increment). In this way, the stress changes may be calculated on the assumption that the total stress increment is elastic. If it can then be determined that yield has been violated, a fictitious stress may be calculated from the plastic strain increment, and subtracted from the stress state which is in violation of yield to give the true stress state.

To see how this is employed in actuality, consider the deviatoric constitutive relation, equation (A-6), in which the deviatoric stress increment is calculated via the product of the modulus and elastic deviatoric strain increment. The linearity of the deviatoric conversion equations implies, for plastic deformation, that:

$$\Delta s_i = C_{ij} (\Delta e_j^t - \Delta e_j^p) \quad (\text{A-14})$$

The deviatoric total strain increment (Δe_j^t) is calculated with the deviatoric conversion equations, based on the total strain increment. The plastic deviatoric strain increment (Δe_j^p) can be decomposed into its total plastic ($\Delta \epsilon_j^p$) and hydrostatic plastic ($\Delta \bar{\epsilon}_j^p$) components, respectively.

The total plastic strain component is necessarily normal to the yield surface, and is given by:

$$\Delta \epsilon_j^p = \Delta \lambda \frac{\partial f}{\partial \sigma_j} \quad (\text{A-15})$$

where f is the equation governing the yield surface, and $\Delta \lambda$ is a proportionality constant for the yield surface normal ($\partial f / \partial \sigma_j$), which has been evaluated at the stress state in question. If one assumes an anisotropic yield condition like Hill's³⁹ in which the yield criterion is independent of the hydrostatic pressure, then the yield surface normal may be evaluated with the use of the deviatoric stresses (e.g., $\partial f / \partial s_j$).

Similarly, the hydrostatic plastic component represents the three components of plastic deviatoric dilatation, and can be explicitly calculated knowing the elastic and plastic material constants and the same proportionality constant $\Delta\lambda$ required above.

As a side note, the usage "plastic dilatation" would seem to imply that plastic incompressibility does not hold. This is, however, not the case. Recall that equations (A-3), (A-7), (A-9), and (A-11) were proven valid only for elastic deformations. The concept of plastic strain was introduced to represent the difference between the elastic and total strain components. This term "plastic dilatation" in fact represents a portion of the total dilatation to be subtracted off to yield the proper value of elastic deviatoric dilatation. The plastic incompressibility relation:

$$\Delta\epsilon_1^P + \Delta\epsilon_2^P + \Delta\epsilon_3^P = 0 \quad (\text{A-16})$$

is still assumed to hold throughout all calculations derived here. Thus, expressing the plastic deviatoric dilatation term as

$$\Delta\bar{\epsilon}_j^P = \frac{d\bar{\epsilon}_j^P}{d\lambda} \Delta\lambda \quad (\text{A-17})$$

the deviatoric constitutive relation may be expressed, using equations (A-14), (A-15), and (A-17) as

$$\Delta s_i = C_{ij} \left(\Delta e_j^t - \left(\frac{\partial f}{\partial s_j} - \frac{d\bar{\epsilon}_j^P}{d\lambda} \right) \Delta\lambda \right) \quad (\text{A-18})$$

Notice that the only term in this relationship which differs from the isotropic case is the last term involving $(d\bar{\epsilon}_j^P/d\lambda)$. This term is zero for the isotropic case because of the fact that there is no dilatation as a result of deviatoric stress. Similarly, this term can not generally be zero for the anisotropic case because equation (A-18) is a deviatoric stress relationship. The term $(d\bar{\epsilon}_j^P/d\lambda)$ is precisely the magnitude required to force the deviator stress to remain in the π plane (i.e., have no hydrostatic components).

The quantity $\Delta\lambda$ may be evaluated by taking the scalar product of equation (A-18) with $(\partial f/\partial s_i)$. Because Δs_i is tangential to the yield surface and $(\partial f/\partial s_i)$ is the yield surface

normal, the scalar product is zero. Similarly the term $(d\bar{\epsilon}_j^P/d\lambda)$ is of a form identical to that resulting from the purely hydrostatic stress state described in equation (A-7). Thus, the quantity $C_{ij}(d\bar{\epsilon}_j^P/d\lambda)$ is parallel with the hydrostat vector. If one assumes an anisotropic yield condition like Hill's³⁹ in which the yield criterion is independent of the hydrostatic pressure, the scalar product of $C_{ij}(d\bar{\epsilon}_j^P/d\lambda)$ and $(\partial f/\partial s_i)$ is also zero. Thus the value for $\Delta\lambda$ may be calculated as:

$$\Delta\lambda = \frac{\frac{\partial f}{\partial s_i} C_{ij} \Delta e_j^t}{\frac{\partial f}{\partial s_i} C_{ij} \frac{\partial f}{\partial s_j}} \quad (\text{A-19})$$

This expression for $\Delta\lambda$ is of a form identical to that obtained for the isotropic case, and can be used in equation (A-18) to calculate the elastic deviatoric stress increment.

Because of the curvature of the yield surface and the fact that $\Delta\lambda$ was calculated for the stress state existing at the beginning of the time cycle, the updated stress state resulting from equation (A-18) may in fact still lie slightly outside the yield surface. What is done at this point in both the existing models and the proposed one is to scale back all the stress components uniformly until the yield surface is exactly reached. Though this technique introduces some error on its own, it is believed that the error is not too great since the components of the increment of stress scale back are nearly normal to the yield surface in many cases. Also, ways have been devised by Vavrick and Johnson⁵¹ to decrease the magnitude of this error. Their techniques employ subdivision of the time cycle. However, some anisotropic formulations use a deviatoric stress formulation in which elastic deviatoric stresses are defined in the following way⁵⁰

$$\Delta s_i = \begin{cases} C_{ij} \Delta \epsilon_j - 3K (\Delta \epsilon_1 + \Delta \epsilon_2 + \Delta \epsilon_3) , & i=1,2,3 \\ C_{ij} \Delta \epsilon_j , & i=4,5,6 \end{cases} \quad (\text{A-13})$$

and additional error is introduced as a result. This occurs because the formulation in equation (A-13) does not guarantee that the sum of the deviatoric stresses will equal zero for an anisotropic material, and in fact they will generally not do so. As a result, any scale back of the stresses employed to meet the yield criterion will include a hydrostatic

component. Such hydrostatic scale back violates basic rules of yield surface normality in a fundamental way. Furthermore, techniques proposed by Vavrck and Johnson which decrease the error resulting from stress scale-back will not decrease the amount of hydrostatic stress error introduced into the calculation as the result of using a formulation like that of equation (A-13).

A.5 Summary.

An anisotropic formulation has been proposed which satisfies the condition of reducing to Hooke's Law/Prandtl Reuss Flow Rule when employing the constraint of constant compressibility and isotropy, but which conveniently allows for anisotropic material properties and variable compressibility.

The deviatoric stress technique which has been used routinely in the isotropic impact codes for describing isotropic behavior has been effectively combined with the anisotropic constitutive relations to produce a truly deviatoric anisotropic constitutive relation. In this deviatoric formulation, deviatoric stress is expressed only in terms of deviatoric strain, and compressibility does not influence the deviatoric relation.

Existing formulations suffer from drawbacks which have been eliminated in the present formulation. Some of the drawbacks of previous formulations may be enumerated as follows:

- a. working with absolute stress and strain offers no simple way to perform calculations involving variable compressibility,
- b. calculating hydrostatic pressure increments (instead of complete hydrostatic pressure) can introduce error associated with obtaining and averaging the tangent bulk modulus over a strain increment (this problem compounded by the fact that Hugoniot data is usually gathered in the form pressure versus dilatation, the slope of which is the tangent bulk modulus), and
- c. use of a "deviatoric" stress which includes a hydrostatic component will produce error in the pressure calculation if stresses are scaled back to satisfy the yield condition.

Additionally, the formulation can be simply coded into existing impact codes which presently use the deviatoric stress technique for isotropic materials. Finally, it is hoped that the formulation provides an enhanced physical interpretation on the behavior of anisotropic materials.

INTENTIONALLY LEFT BLANK.

APPENDIX B:

ANISOTROPY DIRECTION TRACKING FOR
AXISYMMETRIC SIMULATIONS

INTENTIONALLY LEFT BLANK.

APPENDIX B:

ANISOTROPY DIRECTION TRACKING FOR AXISYMMETRIC SIMULATIONS

In order to model anisotropy for axisymmetric code simulations, one must have the ability to accurately track element motion in the θ direction. In particular, one must ascertain the orientation of anisotropy in the r - z plane, as well as the angle formed between the principal direction of anisotropy and the r - z plane.

One of the first problems to be considered is the shape of a computational element which has experienced motion in the θ direction. The data available are the r , z , and θ coordinates for the three nodes at the vertices of the element. A logical choice for an interpolation function for the θ position throughout the element, which is consistent with the r and z interpolations is

$$\theta = \alpha r + \beta z + \gamma \quad , \quad (B-1)$$

where α , β , and γ are constants chosen in such a way that θ , evaluated at each of the nodal vertices, matches that node's coordinate. One of the favorable results of choosing an interpolation function like equation (B-1) is that the element, when plotted in a Cartesian r , z , θ space (Figure B-1) is still flat. However, interpolation function (B-1) suffers drawbacks. In particular, the surface of the element in cylindrical r - z - θ space is curved in such a way that the angle (ϕ) formed between the element surface at a point and the r - z plane through that point varies for the different points in the element. Figure B-2 depicts this behavior schematically where, for simplicity of illustration, projection into the r - θ plane has been performed. As such, the term ϕ' has been employed to represent the angle ϕ as projected into the r - θ plane.

On the other hand, the curved element proposed is much more desirable than say, a flat element in cylindrical r - z - θ space. Only when one admits the possibility of having a curved element can one consider the more realistic situation of having a deformed element curve around the axis of symmetry. As was noted however, in Figure B-2, the angle (ϕ) formed between the deformed element and the r - z plane varies slightly at different points in

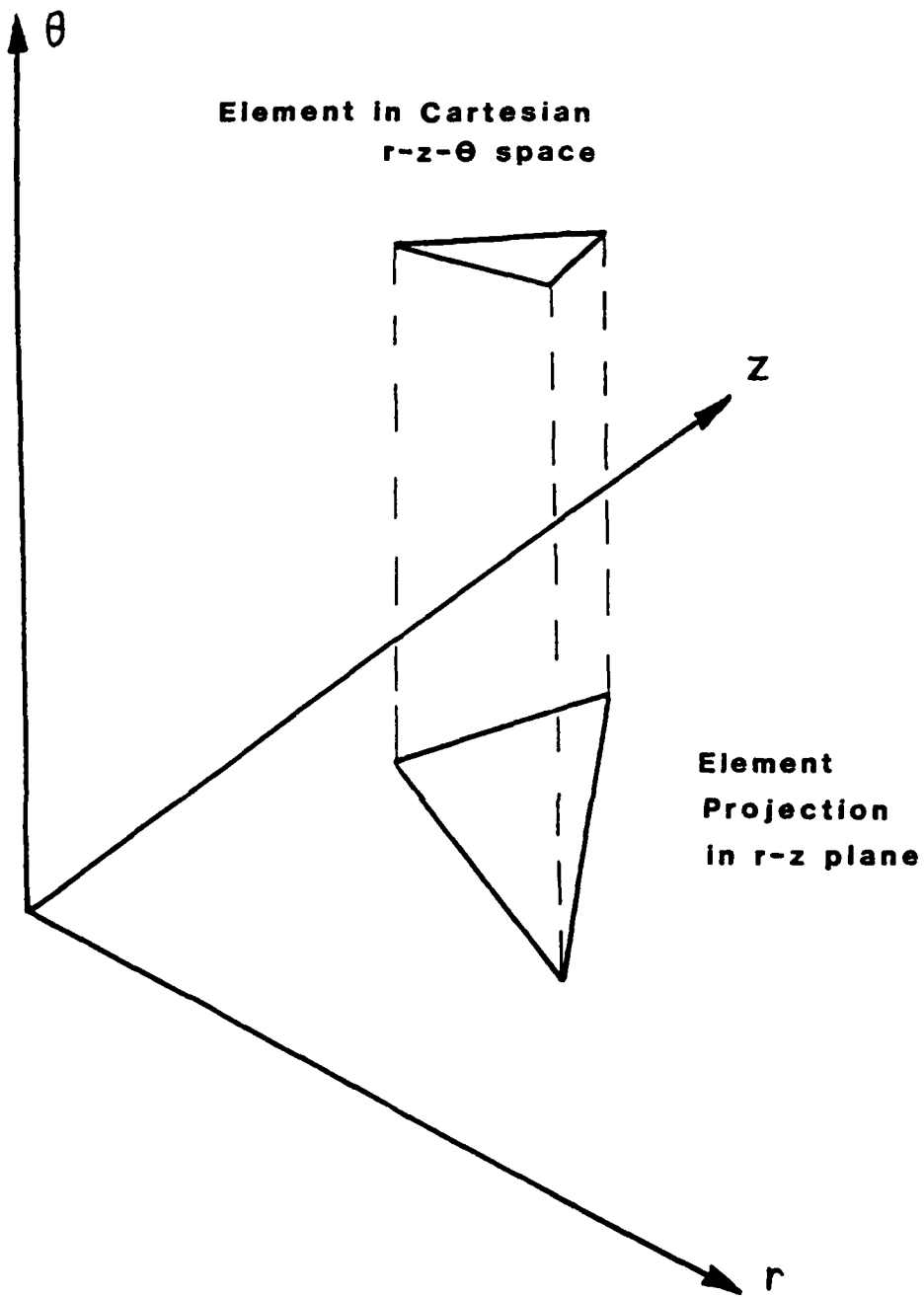
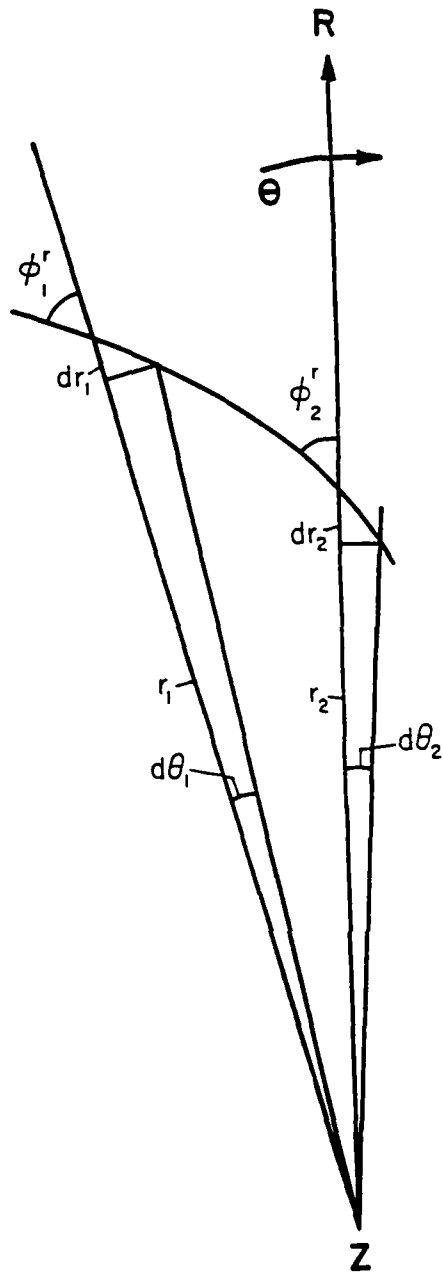


Figure B-1. Interpolation for θ within a computational element is flat in Cartesian r - z - θ space.



$$\theta = \alpha r + \beta z + \gamma$$

$$\frac{d\theta}{dr} = \alpha = \text{constant}$$

$$\frac{d\theta_1}{dr_1} = \frac{d\theta_2}{dr_2} = \frac{d\theta}{dr} = \alpha$$

$$\phi_1^r = \phi_2^r$$

$$\tan \phi_1^r = r_1 \frac{d\theta}{dr}$$

$$\tan \phi_2^r = r_2 \frac{d\theta}{dr}$$

Figure B-2. Schematic depiction of how interpolation function for θ causes the angle between r - z plane and computational element (ϕ') to vary throughout element, as viewed down the z axis in cylindrical r - z - θ space.

the element. A reasonable average for this angle may be obtained by evaluating the angle at the centroid of the element.

The actual situation of anisotropy modeling is further complicated by two issues:

- a. there exists a particular line in the r-z plane, which represents the projection of the principal direction of anisotropy onto the r-z plane; and
- b. at time zero, when an element's geometry is undeformed, there may exist a non-zero angle between the principal direction of anisotropy and the r-z plane.

The orientation of principal direction, as projected into the r-z plane (item 1 above), can be easily tracked by integrating the element's r-z rotation rate. This rotation rate is readily available from standard axisymmetric hydrocode computations. It was shown in Figure B-1 how a deformed element remains flat in the Cartesian r-z- θ space. For the anisotropic problem at hand, one must be able to determine the angle (ϕ) formed between this deformed element and the r-z plane, along a particular direction. In Figure B-3, this direction is shown as a vector dl which forms an angle δ with respect to the r axis, and lies in the r-z plane. To determine $d\theta/dl$, one employs directional derivatives $\partial\theta/\partial r$ and $\partial\theta/\partial z$ so that

$$\frac{d\theta}{dl} = \frac{\partial\theta}{\partial r} \frac{\partial r}{\partial l} + \frac{\partial\theta}{\partial z} \frac{\partial z}{\partial l} \quad (B-2)$$

Recalling equation (B-1), and substituting into equation (B-2), it is seen that $d\theta/dl$ may be expressed as

$$\frac{d\theta}{dl} = \alpha \cos \delta + \beta \sin \delta \quad (B-3)$$

The parameters α and β are easily determinable from vector analysis. If the quantity $V_{12} \times V_{13}$ takes on the value

$$V_{12} \times V_{13} = a \hat{i} + b \hat{j} + c \hat{k} \quad (B-4)$$

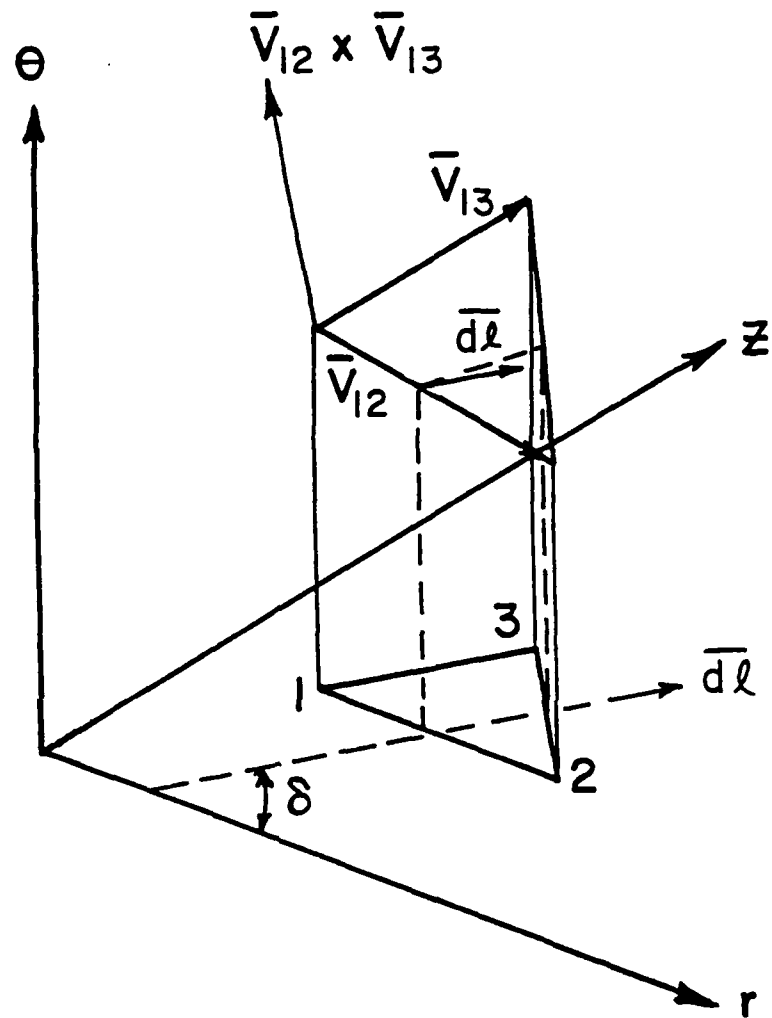


Figure B-3. Computational element viewed in Cartesian r - z - θ space, showing all quantities needed to compute $d\theta/d\ell$, and hence the angle between the r - z plane and deformed element in cylindrical r - z - θ space (ϕ).

then it can be shown that $\alpha = -a/c$ and $\beta = -b/c$. Thus, the angle (ϕ) formed between the element and the r-z plane along the direction dl is given by

$$\tan \phi = r \frac{d\theta}{dl} \quad (B-5)$$

This result is similar to that derived in Figure B-2, except that it accounts for arbitrary directions of anisotropy, and does not assume that dl is aligned with the radial axis.

The final point to be considered is the situation where the principal direction of anisotropy does not lie in the plane of the element (item 2 above). Even if the element does not experience deformation in the θ direction, it is clear that the out of plane angle ϕ may vary with r and z distortion. In particular, an element in the r-z plane stretched infinitely large will have ϕ approach zero, while an element being compressed to infinitesimal proportions will have ϕ approach $\pi/2$. The way that this situation may be addressed computationally is to (within an element) augment the nodes θ coordinates by a fictitious amount only for the purposes of computing ϕ . This fictitious augmentation will be computed in such a fashion as to guarantee that the initial value ϕ takes on is the desired initial value for ϕ . In the absence of this augmentation, the initial value for ϕ would otherwise be zero identically. These augmentation values are computed once at the commencement of computation for each element, and are used throughout the numerical computation.

It has thus been shown that the necessity of tracking anisotropy orientation in axisymmetric elements may be accomplished in a straight forward manner. The tracking is done on two parameters. First, the projection of anisotropy direction on the r-z plane is tracked via r-z element rotation. Secondly, the angle (ϕ) formed between the principal direction of anisotropy and the r-z plane is tracked. The employment of this type of anisotropy tracking permits the effective modeling of anisotropic materials in axisymmetric codes in such a way as to permit anisotropy induced accelerations in the θ direction of the cylindrical coordinate system.

LIST OF SYMBOLS

- ()' a primed variable is a quantity whose value is taken in an arbitrary laboratory reference frame. The same quantities, when unprimed, are those taken in the "material coordinate frame", unless otherwise noted.
- ()^t a superscript t denotes that a variable (e.g., strain) represents a total quantity, which is composed of an elastic part and a plastic part.
- ()^p a superscript p denotes that a variable (e.g., strain) represents a plastic quantity.
- ($\dot{\quad}$) a dotted quantity represent time differentiation.
- $\Delta()$ a upper case delta before a quantity signifies that the quantity is an increment.
- $\delta()$ a lower case delta before a quantity signifies that the quantity is an increment.
- A_{ij} the matrix which, when multiplied by the contracted stress vector, produces the yield surface normal in the material reference frame.
- A_{ij}' the matrix which, when multiplied by the contracted stress vector, produces the yield surface normal in the laboratory reference frame.
- \tilde{A}_{ij} the difference between A_{ij}' and A_{ij} .
- a major axis half-length of anisotropic yield ellipse, or alternately linear acceleration.
- α liner half angle, or alternately an interpolation constant.
- b minor axis half-length of anisotropic yield ellipse.
- β an interpolation constant.

- C_{ij} modulus matrix (6x6) which relates stress increments $d\sigma_i$ to elastic strain increments $d\varepsilon_j$.
- D shaped charge diameter.
- δ thickness of cone or liner element, or alternately the angle formed between the r axis and the projection of a principal material direction onto the r-z plane.
- δm mass of a liner element or jet segment.
- E_i Young's modulus in direction i.
- e_j deviatoric elastic strain components (6 independent). In this report, the term "deviatoric" will imply a deviation from the strain state resulting from a condition of hydrostatic pressure. For anisotropic materials, strain is not uniform under conditions of hydrostatic pressure (i.e. the three principal components of strain are not identical). As a result, the normal deviatoric strain components are NOT simply the difference between the total strain component and the average of the normal strain components.
- \bar{e} deviatoric dilatation ($e_1+e_2+e_3$). Though dilatation is only a function of pressure for isotropic materials, dilatation may vary in an anisotropic material just by varying the deviatoric stress (without changing the pressure). Thus, this dilatation associated with the deviatoric stress is referred to as deviatoric dilatation.
- ε_j elastic strain components in contracted notation; indices 1 to 3 are normal components, whereas 4 to 6 are the shear components 23, 13, and 12 respectively.
- $\bar{\varepsilon}_j$ strain state resulting from hydrostatic pressure. For an isotropic material, the three normal "hydrostatic" strains would be equal. This is not the case for anisotropic material.

- ϵ_t normal strain in the thickness direction of a rotary forged tensile specimen.
- ϵ_w normal strain across the width of a rotary forged tensile specimen.
- F coefficient of Hill's yield criterion.
- f the plastic potential (i.e., yield function) or alternately, the fraction of liner element mass which ends up in a jet segment.
- $\partial f / \partial \sigma_j$ the vector normal to the yield surface given by the function f.
- $\partial f / \partial s_j$ is equivalent to $\partial f / \partial \sigma_j$ for a yield criterion like the Von Mises or Hill, where yielding is not a function of hydrostatic pressure.
- ϕ the angle formed between a distorted computational element and the r-z plane.
- ϕ^r the angle formed between a distorted computational element and the r-z plane, as seen viewing down the z axis.
- G coefficient of Hill's yield criterion.
- G_{ij} Shear modulus in i-j plane.
- Γ the CCW angle of rotation about one of the laboratory axes, from the laboratory coordinate system to the preferred material coordinate system.
- γ an interpolation constant.
- γ_{ij} component of engineering shear strain, equal to twice the tensorial component ϵ_{ij} .
- H coefficient of Hill's yield criterion.

- I polar moment of inertia.
- K_ϵ a parameter which represents the ratio of longitudinal to transverse strain (in the material reference frame) under conditions of hydrostatic pressure ($\sigma_1 = \sigma_2 = \sigma_3$).
- K_σ a parameter which represents the ratio of longitudinal to transverse stress (in the material reference frame) under conditions of uniform strain ($\epsilon_1 = \epsilon_2 = \epsilon_3$).
- k strength of a material in simple shear.
- L coefficient of Hill's yield criterion, or alternately the length of a shaped charge cone.
- l_1 length of anisotropic yield ellipse along the 1 direction.
- l_2 length of anisotropic yield ellipse along the 2 direction.
- l_3 length of anisotropic yield ellipse along the 3 direction.
- dl the vector in the direction of the projection of a principal material axis onto the r-z plane.
- $\Delta\lambda$ a proportionality constant between the yield surface normal vector, and the total plastic strain increment vector, which are parallel.
- M coefficient of Hill's yield criterion, or alternately the mass of a cylinder slice.
- m fractional mass of a cylinder slice, or alternately the cosine of an angle in question.
- N coefficient of Hill's yield criterion.
- n the sine of an angle in question.

\mathbf{n}	outward normal vector to the anisotropic yield ellipse.
ν_{ij}	Poisson's ratio in i-j plane.
$O()$	Signifies the order of magnitude of the quantity in parentheses.
P	angular momentum.
Q_1	a term comprised of Hill's yield constants, equal to N-2H-G.
Q_2	a term comprised of Hill's yield constants, equal to N-2H-F.
Q_3	a term comprised of Hill's yield constants, equal to M-L.
R	Initial radius of a liner element.
r	radial coordinate in cylindrical r-z- θ space, or alternately the so called "r-value" of anisotropic material.
r_j	radius of jet segment.
ρ	density.
s_i	deviatoric elastic stress components (6 independent). In this report, the term "deviatoric" will imply a deviation from the stress state resulting from a condition of hydrostatic pressure.
σ	standard deviation.
σ_i	stress components in contracted notation; indices 1 to 3 are normal components, whereas 4 to 6 are the shear components 23, 13, and 12 respectively.

$\bar{\sigma}$	average stress, by definition equal to the negative of the hydrostatic pressure.
σ_{θ}	normal hoop stress component.
T	torque.
T_{ij}	The transformation matrix which converts stress and strain from one coordinate system to another.
T_0	initial value of torque.
t	time, or alternately tensile specimen thickness.
t_0	original tensile specimen thickness.
$\tau_{r\theta}$	shear stress component in the r- θ plane.
$\tau_{z\theta}$	shear stress component in the z- θ plane.
V_j	axial jet particle velocity.
V_0	initial circumferential velocity component of a liner element.
V_{ij}	the vector connecting node i of a computational element to node j of the same element, where i, j, and k may take on the values 1, 2, and 3.
w	tensile specimen width.
w_0	original tensile specimen width.
Ω	shaped charge spin rate.

Ω	angular velocity of liner element at initial radius R (prior to collapse), as a result of residual stress relief mode 2.
ω	angular velocity of a jet particle, or of the collapsing liner element which forms the jet particle.
ω_{net}	momentum averaged angular velocity through a certain percentage of a collapsing anisotropic cylinder slice.
ω_s	angular velocity of the slug, which results from shaped-charge liner collapse.
$\Delta\xi$	length of a jet segment, originating from a liner element of length Δz .
$Y_{1,2,3}$	normal flow stress in material directions 1, 2, and 3, respectively. For an elastic-perfectly plastic material, it equals the yield strength.
$Y_{4,5,6}$	shear flow stress in the 23, 13, and 12 planes, respectively. For an elastic-perfectly plastic material, it equals the yield strength.
Y_{skew}	normal flow stress for rotary forged tensile tab oriented 45 degrees from both the circumferential and radial directions.
θ	circumferential coordinate in cylindrical r-z- θ space.
z	axial coordinate in cylindrical r-z- θ space.
Δz	axial length of a liner element.

INTENTIONALLY LEFT BLANK.

No of Copies	<u>Organization</u>
(Unclass., unlimited) 12	Administrator
(Unclass., limited) 2	Defense Technical Info Center
(Classified) 2	ATTN: DTIC-DDA Cameron Station Alexandria, VA 22304-6145
1	HQDA (SARD-TR) WASH DC 20310-0001
1	Commander US Army Materiel Command ATTN: AMCDRA-ST 5001 Eisenhower Avenue Alexandria, VA 22333-0001
1	Commander US Army Laboratory Command ATTN: AMSLC-DL Adelphi, MD 20783-1145
2	Commander Armament RD&E Center US Army AMCCOM ATTN: SMCAR-MSI Picatinny Arsenal, NJ 07806-5000
2	Commander Armament RD&E Center US Army AMCCOM ATTN: SMCAR-TDC Picatinny Arsenal, NJ 07806-5000
1	Director Benet Weapons Laboratory Armament RD&E Center US Army AMCCOM ATTN: SMCAR-CCB-TL Watervliet, NY 12189-4050
1	Commander US Army Armament, Munitions and Chemical Command ATTN: SMCAR-ESP-L Rock Island, IL 61299-5000
1	Commander US Army Aviation Systems Command ATTN: AMSAV-DACL 4300 Goodfellow Blvd. St. Louis, MO 63120-1798
1	Director US Army Aviation Research and Technology Activity Ames Research Center Moffett Field, CA 94035-1099

No of Copies	<u>Organization</u>
1	Commander US Army Missile Command ATTN: AMSMI-RD-CS-R (DOC) Redstone Arsenal, AL 35898-5010
1	Commander US Army Tank-Automotive Command ATTN: AMSTA-TSL (Technical Library) Warren, MI 48397-5000
1	Director US Army TRADOC Analysis Command ATTN: ATAA-SL White Sands Missile Range, NM 88002-5502
(Class. only) 1	Commandant US Army Infantry School ATTN: ATSH-CD (Security Mgr.) Fort Benning, GA 31905-5660
(Unclass. only) 1	Commandant US Army Infantry School ATTN: ATSH-CD-CSO-OR Fort Benning, GA 31905-5660
1	Air Force Armament Laboratory ATTN: AFATL/DLODL Eglin AFB, FL 32542-5000
	<u>Aberdeen Proving Ground</u> Dir, USAMSAA ATTN: AMXSY-D AMXSY-MP, H. Cohen Cdr, USATECOM ATTN: AMSTE-TO-F Cdr, CRDEC, AMCCOM ATTN: SMCCR-RSP-A SMCCR-MU SMCCR-MSI Dir, VLAMO ATTN: AMSLC-VL-D

<u>No. of Copies</u>	<u>Organization</u>	<u>No. of Copies</u>	<u>Organization</u>
2	Director DARPA ATTN: J. Richardson Maj. R. Lundberg 1400 Wilson Blvd. Arlington, VA 22209-2308	2	Naval Weapons Support Center ATTN: John D. Barber Sung Y. Kim Code 2024 Crane, IN 47522-5020
1	Defense Nuclear Agency ATTN: Maj. James Lyon 6801 Telegraph Rd. Alexandria, VA 22192	6	Naval Surface Warfare Center ATTN: Charles R. Garnett (Code G-22) Linda F. Williams (Code G-33) Joseph C. Monolo (Code G-34) Larry Crabtree (Code G-34) Janet Vena (Code G-34) Mary Jane Sill (Code H-11) Dahlgren, VA 22448-5000
1	US Army Strategic Defense Command ATTN: CSSD-H-LL (Tim Cowles) Huntsville, AL 35807-3801	15	Naval Surface Warfare Center ATTN: Pao C. Huang (G-402) Bryan A. Baudler (R-12) Robert H. Moffett (R-12) Robert Garrett (R-12) Thomas L. Jungling (R-32) Philip Marshall (U-11) Windsor Furr (U-11) Daniel Harris (U-11) Amos A. Dare (U-12) Richard Caminity (U-43) John P. Matra Paula Walter Lisa Mensi Kenneth Kiddy F.J. Zerilli 10901 New Hampshire Ave. Silver Spring, MD 20903-5000
1	USA ARMC ATTN: ATSB-CD (Dale Stewart) Ft. Knox, KY 40121	1	Naval Civil Engr. Lab. ATTN: Joel Young (Code L-56) Port Hueneme, CA 93043
1	US Army MICOM ATTN: AMSMI-RD-TE-F (Matt H. Triplett) Redstone Arsenal, AL 35898-5250	4	Air Force Armament Lab. ATTN: AFATL/DLJW (W. Cook) AFATL/DLJW (M. Nixon) AFATL/MNW (Lt. Donald Lorey) AFATL/MNW (Richard D. Guba) Eglin AFB, FL 32542
2	TACOM RD&E Center ATTN: AMCPM-ABMS-SA (John Rowe) AMSTA-RSS (K.D. Bishnoi) Warren, MI 48397-5000	2	MSD/ENL ATTN: W. Dyess I. Talbot Eglin, AFB 32542-5000
2	Commander Armament RD&E Center US Army AMCCOM ATTN: SMCAR-CCH-V (M.D. Nicolich) SMCAR-FSA-E (W.P. Dunn) Picatinny Arsenal, NJ 07806-5000	1	3246 Test Wing/TZFT ATTN: Cpt. Mark Olson Eglin AFB, FL 32542-5000
4	US Army Belvoir RD&E Center ATTN: STRBE-NAE (Bryan Westlich) STRBE-JMC (Terilee Hanshaw) STRBE-NAN (Steven G. Bishop) STRBE-NAN (Josh Williams) Ft. Belvoir, VA 22060-5166		
1	USMC/MCRDAC/PM Grounds Wpns. Br. ATTN: Dan Haywood Firepower Div. Quantico, VA 22134		
3	Naval Weapons Center ATTN: Tucker T. Yee (Code 3263) Don Thompson (Code 3268) W.J. McCarter (Code 6214) China Lake, CA 93555		

<u>No. of Copies</u>	<u>Organization</u>	<u>No. of Copies</u>	<u>Organization</u>
8	Sandia National Laboratory ATTN: Robert O. Nellums (Div. 9122) Jim Hickerson (Div. 9122) Marlin Kipp (Div. 1533) Allen Robinson Div. 1533) Wm. J. Andrzejewski (Div. 2512) Don Marchi (Div. 2512) R. Graham (Div. 1551) R. Lafarge (Div. 1551) P.O. Box 5800 Albuquerque, NM 87185	2	Explosive Technology ATTN: James Kennedy Michael L. Knaebel P.O. Box KK Fairfield, CA 94533
10	Director Los Alamos National Laboratory ATTN: G.E. Cort (MS K574) Tony Rollett (MS K574) Mike Burkett (MS K574) Robert Karpp (MS P940) Rudy Henninger (MS K557, N-6) Robert M. Gates (MS K574) Roy Greiner (MS-G740) James P. Ritchie (B214, T-14) John Bolstad (MS G787) Bill Harvey P.O. Box 1663 Los Alamos, NM 87545	2	Rockwell Missile Systems Div. ATTN: Terry Neuhart Dennis Kaisand 1800 Satellite Blvd. Duluth, GA 30136
13	Lawrence Livermore National Laboratories ATTN: Barry R. Bowman (L-122) Ward Dixon (L-122) Raymond Pierce (L-122) Russell Rosinsky (L-122) Owen J. Alford (L-122) Diana Stewart (L-122) Tony Vidlak (L-122) Albert Holt (L-290) John E. Reaugh (L-290) David Wood (L-352) Robert M. Kuklo (L-874) Thomas McAbee (MS 35) Michael J. Murphy P.O. Box 808 Livermore, CA 94550	1	Rockwell Intl./Rocketdyne Div. ATTN: James Moldenhauer 6633 Canoga Ave (HB 23) Canoga Park, CA 91303
1	Battelle Northwest ATTN: John B. Brown, Jr. MSIN 3 K5-22 P.O. Box 999 Richland, WA 99352	1	IIT Research Institute ATTN: Gerard Koller 10 W. 35th St. Chicago, IL 60616
1	Advanced Technology, Inc. ATTN: John Adams P.O. Box 125 Dahlgren, VA 22448-0125	1	Allied Signal ATTN: L. Lin P.O. Box 31 Petersburg, VA 23804
		2	McDonnell-Douglas Helicopter ATTN: Loren R. Bird Lawrence A. Mason 5000 E. McDowell Rd. (MS 543-D216) Mesa, AZ 85205
		1	University of Colorado Campus Box 431 (NNT 3-41) ATTN: Timothy Maclay Boulder, CO 80309
		1	New Mexico Inst. Mining & Tech. Campus Station (TERA Group) ATTN: David J. Chavez Socorro, NM 87801
		2	Schlumberger Perforating & Test ATTN: Manuel T. Gonzalez Dan Markel P.O. Box 1590/14910 Ariline Rd. Rosharon, TX 77583-1590
		2	Aerojet Ordnance/Exp. Tech. Ctr. ATTN: Patrick Wolf Gregg Padgett 1100 Bulloch Blvd. Socorro, NM 87801

<u>No. of Copies</u>	<u>Organization</u>
1	Aerojet Precision Weapons Dept. 5131/T-W ATTN: Robert S. Kowell 1100 Hollyvale Azusa, CA 91702
1	Aerojet Ordnance Corporation ATTN: J. Carleone 2521 Michelle Drive Tustin, CA 92680
1	Babcock & Wilcox ATTN: Ken Camplin P.O. Box 11165 Lynchburg, VA 24506
2	Physics International ATTN: Ron Funston Lamont Garnett 2700 Merced St./P.O. Box 5010 San Leandro, CA 94577
1	Sparta ATTN: Tony Hill 5401 East La Palma Ave. Anaheim, CA 92807
2	Lockheed Missile & Space Co., Inc. ATTN: S. Kusumi (O-81-11, Bldg. 157) Jack Philips (O-54-50) P.O. Box 3504 Sunnyvale, CA 94088
1	Lockheed Missile & Space Co., Inc. ATTN: Richard A. Hoffman Santa Cruz Fac./Empire Grade Rd. Santa Cruz, CA 95060
1	Boeing Corporation ATTN: Thomas M. Murray (MS 84-84) P.O. Box 3999 Seattle, WA 98124
2	Mason & Hanger - Silas Mason Co. ATTN: Thomas J. Rowan Christopher Vogt Iowa Army Ammunition Plant Middletown, IA 52638-9701
1	Nuclear Metals Inc. ATTN: Jeff Schreiber 2229 Main St. Concord, MA 01742

<u>No. of Copies</u>	<u>Organizaion</u>
2	Dyna East Corporation ATTN: P.C. Chou R. Ciccarelli 3201 Arch St. Philadelphia, PA 19104
2	Southwest Research Institute ATTN: C. Anderson A. Wenzel 6220 Culebra Road P.O. Drawer 28510 San Antonio, TX 78284
2	Battelle - Columbus Laboratories ATTN: R. Jameson S. Golaski 505 King Avenue Columbus, OH 43201
3	Honeywell, Inc. ATTN: Gordon R. Johnson Tim Holmquist Kuo Chang MN 48-2700 7225 Northland Dr. Brooklyn Park, MN 55428
1	AAI Corp. ATTN: Richard Huffman Dept. 403/Bldg. 100 Hunt Valley, MD 21030
5	LTV Missiles & Electronics Group ATTN: Gary Hough (WT-50) G.L. Jackson (WT-71) M.M. Tower (WT-78) Ken Havens (EM-36) R.J. Taylor (EM-36) P.O. Box 65003 Dallas, TX 75265-0003
2	General Research Corp. ATTN: Alex Charters Tom Menna 5383 Hollister Ave. Santa Barbara, CA 93160-6770
1	General Dynamics ATTN: Jaime Cuadros P.O. Box 50-800 Mail Zone 601-87 Ontario, CA 91761-1085
1	Systems, Science and Software, Inc. ATTN: R. Sedgwick 3398 Carmel Mountain Rd. San Diego, CA 92121

<u>No. of Copies</u>	<u>Organization</u>
2	California Research & Tech. Corp. ATTN: Roland Franzen Dennis Orphal 5117 Johnson Dr. Pleasanton, CA 94566
2	Orlando Technology, Inc. ATTN: Dan Matuska J. Osborn P.O. Box 855 Shalimar, FL 32579
3	Kaman Sciences Corporation ATTN: D. Barnette D. Elder P. Russell P.O. Box 7463 Colorado Springs, CO 80933

<u>No. of Copies</u>	<u>Organization</u>	<u>No. of Copies</u>	<u>Organization</u>
2	Defense Research Establishment Suffield ATTN: Chris Weickert David MacKay Ralston, Alberta, TOJ 2NO Ralston CANADA	1	Centre d'Etudes de Gramat ATTN: SOLVE Gerald 46500 Gramat FRANCE
1	Defense Research Establishment Valcartier ATTN: Norbert Gass P.O. Box 8800 Courcellette, PQ, GOA 1RO CANADA	1	Centre d'Etudes de Vaujours ATTN: PLOTARD Jean-Paul Boite Postale No. 7 77181 Country FRANCE
1	Canadian Arsenals, LTD ATTN: Pierre Pelletier 5 Montee des Arsenaux Villie de Gardeur, PQ, J5Z2 CANADA	1	PRB S.A. ATTN: M. Vansnick Avenue de Tervueren 168, Bte. 7 Brussels, B-1150 BELGIUM
1	Ernst Mach Institute ATTN: A.J. Stulp Eckerstrasse 4 D-7800 Freiburg i. Br. WEST GERMANY	1	AB Bofors/Ammunition Division ATTN: Jan Hasslid BOX 900 S-691 80 Bofors SWEDEN
1	MBB ATTN: Manfred Held Postfach 1340 D-8898 Schrobenhausen WEST GERMANY		
3	IABG ATTN: H.J. Raatschen W. Schütke F. Scharppf Einsteinstrasse 20 D-8012 Ottobrun b. Muenchen WEST GERMANY		
1	Royal Armament R&D Establishment ATTN: Ian Cullis Fort Halstead Sevenoaks, Kent TN14 7BP ENGLAND		
2	Royal Ordnance ATTN: Chris Constantinou R.C. Davies Euxton Lane, Euxton, Chorley Lancashire PR7 6AD ENGLAND		

USER EVALUATION SHEET/CHANGE OF ADDRESS

This Laboratory undertakes a continuing effort to improve the quality of the reports it publishes. Your comments/answers to the items/questions below will aid us in our efforts.

1. BRL Report Number BRL_TR-3090 Date of Report MAR 90

2. Date Report Received _____

3. Does this report satisfy a need? (Comment on purpose, related project, or other area of interest for which the report will be used.) _____

4. Specifically, how is the report being used? (Information source, design data, procedure, source of ideas, etc.) _____

5. Has the information in this report led to any quantitative savings as far as man-hours or dollars saved, operating costs avoided, or efficiencies achieved, etc? If so, please elaborate. _____

6. General Comments. What do you think should be changed to improve future reports? (Indicate changes to organization, technical content, format, etc.) _____

CURRENT
ADDRESS

Name

Organization

Address

City, State, Zip Code

If indicating a Change of Address or Address Correction, please provide the New or Correct Address in Block 6 above and the Old or Incorrect address below.

OLD
ADDRESS

Name

Organization

Address

City, State, Zip Code

-----FOLD HERE-----

DEPARTMENT OF THE ARMY

Director
U.S. Army Ballistic Research Laboratory
ATTN: SLCBR-DD-T
Aberdeen Proving Ground, MD 21005-9989
OFFICIAL BUSINESS



NO POSTAGE
NECESSARY
IF MAILED
IN THE
UNITED STATES

BUSINESS REPLY MAIL
FIRST CLASS PERMIT No 0001, APG, MD

POSTAGE WILL BE PAID BY ADDRESSEE

Director
U.S. Army Ballistic Research Laboratory
ATTN: SLCBR-DD-T
Aberdeen Proving Ground, MD 21005-9989

-----FOLD HERE-----



**END
FILMED**

DATE:

5-90

DTIC